COMPARISON OF THE NUMERICAL INTEGRATION TECHNIQUE AND THE FINITE ELEMENT METHOD IN THE ANALYSIS OF THIN-SHELL STRUCTURES

J. LESTINGI

Department of Civil Engineering, College of Engineering The University of Akron, Akron, Ohio 44351, U.S.A.

S. BROWN, Jr.

Nuclear Equipment Division, The Babcock and Wilcox Company, Barberton, Ohio, U.S.A.

SUMMARY

The multisegment numerical integration technique and the finite element method are compared for a variety of shell of revolution problems. The advantages and disadvantages of the finite difference, finite element, and multisegment numerical integration method are discussed.

A brief description of the numerical integration technique and its relationship to the direct stiffness procedures is given. It is shown that this combination yields a powerful analytical tool for a wide range of shell of revolution problems.

A numerical study on the effect of segmentation, shell thickness, and Fourier load harmonic on the manipulation error shows that (1) more segments are required for thinner shells; (2) higher harmonics require a greater number of segments; (3) results for calculations on the CDC 6600 are superior to those on the IBM 370/155; (4) in most analyses the number of segments required for an accurate solution need not be large.

Analytical and experimental results for a 3-inch, 1 ply type 321 stainless steel formed bellows show that the numerical integration procedure when combined with a precise mathematical modeling procedure yields highly accurate results.

A comparison between the numerical integration technique and the finite element method for a variable thickness seal subjected to an axisymmetric loading indicates that both analyses produce the same results provided that the analysis is being conducted in accordance with the ASME code requirements where primary and secondary stresses are required and peak stresses need not be calculated.

A hemispherical head with a nozzle subjected to a moment was analyzed by both numerical integration and the finite element method. Both results compare well with existing theoretical and experimental data.

The last example consists of a relatively thick flange subjected to a moment. The response of both models compare favorably and the linearized finite element results are identical to those of the numerical integration method.

Through a series of examples, the authors show that the numerical integration technique handles a broad range of shell configurations and loading conditions. It is found that even for complex seals where it is sufficient to only define the linear stress values for the ASME code requirements, the numerical integration technique provides economical model construction and execution time. It is also shown that in many applications, mesh generation requirements of the finite element method generally exceed those of the numerical integration technique.

INTRODUCTION

The analysis of orthotropic shells of revolution subjected to mechanical and thermal loadings has been the subject of many investigations. Bushnell [1] surveyed the various techniques and computer programs which have been developed for the analyses of these structures. The American Society of Mechanical Engineers has sponsored several seminars on the subject of computer programs in pressure vessel analysis [2], [3], [4].

As one reviews the vast amount of literature and programs available for thin shell analysis, the following questions usually arise: (1) is there a single program which will handle all types of shell analyses; (2) if more than one program is available for shell analysis, is one better than another in certain circumstances; (3) is there a difference in the amount of time needed to learn how to use the programs; (4) is there a difference in the costs involved in setting up problems; (5) how accurate is the solution and how does one determine this.

The purpose of this paper is to attempt to answer some of the above questions. The authors have been involved in the development of programs using the numerical integration technique as well as in the extensive use of ABSA [5] - Axisymmetric and Plane Body Stress Analysis which is based on the work of Wilson [6], ALAS [7] - Asymmetrically Loaded Axisymmetric Solids which is based on the work of Hermann [8], MONSASTF - Multilayered Orthotropic Nonsymmetric Shell Analysis - Stiffness which is based on the numerical integration technique as presented by Kalnins [9], and Cohen [10], and SAVE SS-2 [11] which is based on SEAL SHELL-2 [12].

DISCUSSION OF VARIOUS METHODS

Before proceeding to a discussion and comparison of numerical results, we list here some items which should be considered when one is attempting to assess the applicability and reliability of various methods of analysis. We briefly comment on the major methods of analysis i.e., the finite difference, numerical integration and the finite element method, which have been incorporated into computer programs by many individuals and companies. Generally speaking, the finite difference procedures are not self-checking, i.e, an analyst must choose the mesh spacing to perform the analysis. It is never known whether the mesh spacing is adequate until subsequent mesh sizes are used in the analysis and the results compared. The numerical integration procedure eliminates the uncertainty of the finite difference procedures since the method is self-checking. This occurs since the results are calculated in two distinct ways in the normal calculation procedure. If the results are not the same for the two calculations, there can only be two reasons; either the input is incorrect or the number of segments is not sufficient. These deficiences can be eliminated by having the computer program check all input data for consistency and determine the number of segments. Assuming that such a program exists, the multisegment procedure is still inadequate for a general type analysis, since its basic formulation is for the series type shell. This in effect only allows the shell to be supported at the ends and does not permit intermediate points to be supported or displaced. Of course, it is possible to develop appropriate Gaussian elimination procedures to handle these cases, but it is not a straight forward adaptation of the basic multisegment procedures. The finite element method eliminates the basic drawback of the multisegment numerical integration procedure since it deals with the stiffness of individual segments which can be incorporated into an overall joint stiffness matrix in a very straight forward manner. Thus, the basic problem of the multisegment

procedure is eliminated by the finite element method in that the geometry of the shell can be rather arbitrary. Although it may appear that the finite element method can adequately solve all shell of revolution problems, it is important to note that some problems also exist in this method. In the finite element method, the stiffness matrix is normally developed by assuming within the element a displacement field with undetermined coefficients and then using energy minimization in the determination of the coefficients. Thus, it is seen that the accuracy of the element or segment stiffness matrix depends on the choice of the displacement field. Consequently, the analyst may have accurate answers in some analyses and in others he may not. In addition, a convergence check must be made to determine the adequacy of the number of segments used in the analysis. None of the formulations described above contains all of the features necessary or desirable for the accurate solution of an orthotropic multilayered branch shell of revolution subjected to static mechanical and thermal loadings.

NUMERICAL INTEGRATION AND DIRECT STIFFNESS

We now briefly describe procedures which make use of (i) the accuracy and self-checking features of the multisegment method and (ii) the versatility of the direct stiffness concepts of the finite element method.

The basic equations used in the program MONSASTF are due to Love-Reissner [13]. In place of the isotropic constitutive relations, those for a multilayered orthotropic material are used. The reader is referred to Reference 14 for a summary of the equations.

Once the shell equilibrium, strain displacement and constitutive equations are reduced to fundamental form, the relationship between fundamental variables at two points x_i and x_{i+1} along the shell meridian can be obtained from

$$\underset{\sim}{y}(x_{i+1}) = \underset{\sim}{F}(x_{i+1})\,\underset{\sim}{y}(x_i) + \underset{\sim}{z}(x_{i+1}) \tag{1}$$

where

$$\underset{\sim}{y} = \{w,\ u_\phi,\ \beta_\phi,\ u_\theta,\ Q,\ N_\phi,\ M_\phi,\ N\} \tag{2}$$

such that $\underset{\sim}{F}$ and $\underset{\sim}{z}$ are respectively the fundamental matrix and the particular solution. $\underset{\sim}{F}(x_{i+1})$ is obtained by integrating the set of governing equations from x_i to x_{i+1} eight times (six for symmetric loadings), each time using as the initial conditions a column of the identity matrix and suppressing the mechanical loads to zero. The particular solution $\underset{\sim}{z}(x_{i+1})$ is obtained by integrating the entire set of equations from x_i to x_{i+1} using at x_i the null vector as the initial conditions.

The multisegment method of analysis, which is based on the equations given in [14] and a Gaussian elimination procedure [9], is well suited for the analysis of series type shells which are only supported at the ends. For the analysis of branch shells of revolution with arbitrary support characteristics, the Gaussian elimination procedure either has to be modified or the fundamental matrix can be transformed into a stiffness matrix for a shell segment such that the standard direct stiffness method of analysis can be employed.

Since the stiffness coefficients are the actions which result when one displacement is unity and the remaining are suppressed to zero, the actions $\underset{\sim}{a}_m(x_i)$ and $\underset{\sim}{a}_m(x_{i+1})$ must be expressed in terms of the displacements $\underset{\sim}{d}_m(x_i)$ and $\underset{\sim}{d}_m(x_{i+1})$. Equation (1) can be partitioned and expanded such that the actions are given in terms of the displacements in the form

$$\begin{bmatrix} \underset{\sim}{a}_m(x_i) \\ \hline \underset{\sim}{a}_m(x_{i+1}) \end{bmatrix} = \left[\begin{array}{c|c} -\underset{\sim}{F}_{12}^{-1}\ \underset{\sim}{F}_{11} & \underset{\sim}{F}_{12}^{-1} \\ \hline \underset{\sim}{F}_{21} - \underset{\sim}{F}_{22}\ \underset{\sim}{F}_{12}^{-1}\ \underset{\sim}{F}_{11} & \underset{\sim}{F}_{22}\ \underset{\sim}{F}_{22}^{-1} \end{array}\right] \begin{bmatrix} \underset{\sim}{d}_m(x_i) \\ \hline \underset{\sim}{d}_m(x_{i+1}) \end{bmatrix} - \begin{bmatrix} \underset{\sim}{F}_{12}^{-1}\ \underset{\sim}{z}_{11}(x_{i+1}) \\ \hline \underset{\sim}{F}_{22}\ \underset{\sim}{F}_{12}^{-1}\ \underset{\sim}{z}_{11}(x_{i+1}) - \underset{\sim}{z}_{21}(x_{i+1}) \end{bmatrix} \tag{3}$$

To determine the stiffness coefficients, the second term on the right hand side of equation (3) is deleted and the displacement vector is given values of the columns of the identity matrix. Each resulting action vector constitutes a column of the stiffness matrix yielding for the segment stiffness matrix

$$\underset{\sim}{S}_m = \left[\begin{array}{c|c} -\underset{\sim}{F}_{12}^{-1}\ \underset{\sim}{F}_{11} & \underset{\sim}{F}_{12}^{-1} \\ \hline \underset{\sim}{F}_{21} - \underset{\sim}{F}_{22}\ \underset{\sim}{F}_{12}^{-1}\ F_{11} & \underset{\sim}{F}_{22}\ \underset{\sim}{F}_{12}^{-1} \end{array}\right] \tag{4}$$

With equation (4) the overall joint stiffness matrix can be formed according to the usual procedures of the direct stiffness method of analysis.

To complete the analysis, the fixed end actions due to mechanical and thermal loadings are now developed. This is accomplished by letting $\underset{\sim}{d}_m(x_i) = \underset{\sim}{d}_m(x_{i+1}) = 0$ in equation (3), which yields

$$\underset{\sim}{a}_{mL} = -\begin{bmatrix} \underset{\sim}{F}_{12}^{-1}\ \underset{\sim}{z}_{11}(x_{i+1}) \\ \hline \underset{\sim}{F}_{22}\ \underset{\sim}{F}_{12}^{-1}\ \underset{\sim}{z}_{11}(x_{i+1}) - \underset{\sim}{z}_{21}(x_{i+1}) \end{bmatrix}$$

The solution procedure just outlined has the inherent feature which not only permits the shell to have an arbitrary meridional shape, but also possesses numerical capabilities summarized by:

1. Fully orthotropic materials
2. Arbitrary branch shells with intermediate supports which are handled in a routine manner
3. Meridional variations in the material properties and wall thickness are permitted
4. The shell can be subjected to arbitrary joint loads and displacements
5. Layered shells are treated in the manner of Kalnins [9].

EXAMPLES

In using the MONSASTF program, it is necessary to specify the number of segments into which the shell is divided. To obtain some measure of this as well as the influence of shell thickness and Fourier load harmonic on the manipulation error in the solution, a cantilever cylindrical shell of 10 inch radius and 20 inch length with a radial end load of 10 cosn θ was analyzed for n = 0, 1, 2. The shell was divided into 5, 10, 20, 40, 100, and 200 segments and calculations were performed for thicknesses of 0.2, 0.05 and 0.01 inches. Young's modulus was taken as 10^7 psi and Poisson's ratio as 0.3.

Tables 1, 2 and 3 give the axial and radial deflection at the free end for thicknesses

of 0.2, 0.05 and 0.01 inches, respectively as a function of the Fourier harmonic number and number of segments. The results clearly show

(1) More segments are required for thinner shells than thicker shells.
(2) The higher the harmonic, the greater the number of segments required.
(3) The results for the larger word machine, CDC 6600, are superior to those for the smaller word machine, IBM 370/155.
(4) Manipulation error is apparent in the results obtained on the IBM 370/155 for all values of thickness.
(5) Manipulation error becomes more significant for thinner shells even for calculations on the CDC 6600.

Although the results indicate that manipulation error occurs regardless of the word size, it is important to note that no advantage is gained by using a large number of segments in an analysis. In fact, since the multisegment numerical integration procedure produces answers at joints by two different calculation procedures, it is possible to determine whether the number of segments used is sufficient.

Klein [15] conducted a similar study using a finite element analysis and showed similar trends as those obtained here. Experience with numerical integration procedures has shown that large numbers of segments are not required for an accurate solution. Thus, manipulation error should not play an important role even when the computer program is run on a machine with a relatively short word length.

The numerical integration technique has also been used in the nonlinear bending analysis of thin elastic shells of revolution. NONLIN, which is based on work described in [16], has been applied to the analysis of formed and welded metallic bellows and diaphragms [17]. Figure 1 shows an encapsulated 3-inch, 1-ply formed bellows of type 321 stainless steel. Figure 2 is the mathematical model which was obtained from detailed measurements made on the encapsulated model. The thickness variation for the mathematical model is given in Figure 3. The circled points indicate the measured values while the solid line shows the variation used in the analysis.

Using program NONLIN, the stress state throughout the convolution was determined for an axial compression and internal pressure. Table 4 gives a comparison of the theoretically determined and experimentally determined stresses for an axial compression of 0.060 inch and an internal pressure of 50 psi. The results clearly show that the multisegment procedure adequately predicts the stress state in a shell which has a non-uniform shape and thickness characteristics. The reader is referred to[17] and [18] for more details on the use of NONLIN in bellows and diaphragm analysis.

In addition to seals of the bellows type, variable thickness seals of rather complex contouring are found in nuclear component applications. An example of such a configuration is the ESSE (exit stop-system efflux) seal illustrated in Figure 5. Extensive analyses of such seals are directed to definition of linear membrane, bending stress, and peak stresses or "stress risers". Three models of the seal are presented in Figures 4 and 5 where Figure 4 is SAVE SS-2 representation, and Figure 5 shows the finite element and superimposed MONSASTF model. The SAVE SS-2 model is included here to illustrate earlier types of model constructions extensively used in shell analyses. Of course, considerable improvements have been incorporated into many shell programs to afford improved modeling. The finite element mesh consists of 785 constant strain elements and the MONSASTF representation utilizes ten

shell parts. The three models were subjected to an internal test pressure with fixed boundary conditions at A and B. The outside surface longitudinal stress is shown in Figure 6 for the three models. The values from the finite element program ABSA were linearized by a procedure [19] incorporated into the program. The results in Figure 6 show that good agreement exists between the ABSA and MONSASTF results. SAVE SS-2 stress deviations occur in regions of rapid thickness variations. The computer run time for MONSASTF, SAVE SS-2, and ABSA were approximately T, 2T, and 6T respectively.

Thus far, the problems presented have been concerned with axisymmetric loading of shells of revolution. However, asymmetrically loaded axisymmetric shells may be analyzed in a routine manner by MONSASTF which utilizes a Fourier series representation to evaluate the response of the structure. A particular area of interest has been the study of pipes and nozzles intersecting a shell or plate subjected to moments and transverse loads [20], [21]. In Figure 7, the MONSASTF and ALAS simulation of a hemisphere with an attached nozzle, as constructed in experiments performed by Dally [21] is presented. The ALAS model consisted of 273 elements and the MONSASTF model of 3 parts. Although the weld bead is not included in either model it can be included rather easily in either program. A comparison of the ALAS, MONSASTF, and experimental data in Figure 8 indicates relatively good agreement; maximum deviations occur in the area of the nozzle-shell juncture. It is of some interest to note that in comparing the theoretical Bijlaard [20] and experimental data [21] to the MONSASTF values, the radial moment M_r and force N_r fell within the experimental and Bijlaard results and the N_θ and M_θ from MONSASTF tended to coincide with Bijlaard's results.

The ALAS results indicate significant deviation from the experimental outside σ_θ stress as did the MONSASTF results. The stress points for the ALAS model which oscillate slightly in the juncture region are due to the inclusion of triangular elements and node stress interpolation. The computer run times for both models were approximately equal.

In Figure 9, an ALAS and MONSASTF model of a wide flange which has a diameter to thickness ratio of approximately 14 is presented. The ALAS model consists of 100 elements while the MONSASTF model employs three parts. A moment loading is simulated by a cosine vertical load on both models. The longitudinal stress distribution along the inside and outside surfaces are given in Figure 10. It should be noted that the ALAS stresses are not linearized as they were in the ESSE seal. An evaluation of the equivalent linear stress distribution through the thickness indicates that the ALAS and MONSASTF values are essentially identical within the torus region.

CONCLUSIONS

The problems presented demonstrate the broad range of shell configurations and loading conditions that may be handled by the numerical integration method. The finite element method certainly has been found to be a powerful tool, particularly in defining stress risers in such thin shells as the ESSE seal. However, even for ESSE type seals when it is sufficient to only define the linear stress values for ASME code requirements, the numerical integration technique provides economical model construction and execution time. In problems where finite element refinement is not necessary and computer run time is comparable to numerical integration, it is found that the mesh generation requirements of the finite element method generally exceed those of the numerical integration technique.

REFERENCES

1. D. Bushnell, Computer Analysis of Shell Structures, ASME, 69-WA/PVP-13 (1969).
2. H. Kraus (Editor), Use of the Computer in Pressure Vessel Analysis, ASME Computer Seminar, Dallas, Texas (1968).
3. First International Conference, Pressure Vessel Technology, Part 1 - Design and Analysis, Delft, The Netherlands, (1969).
4. P. V. Marcal (Editor), On General Purpose Finite Element Computer Programs, ASME, N. Y. (1970).
5. J. M. Duke and D. B. VanFossen, Axisymmetric and Plane Body Stress Analysis, The Babcock and Wilcox Research Center Report 79-18, Alliance, Ohio (1969).
6. E. L. Wilson, Structural Analysis of Axisymmetric Solids, AIAA J., 3, 2269-2274 (1965).
7. ALAS User's Manual, The Babcock and Wilcox Company Report 91383, Barberton, Ohio (1971).
8. L. R. Hermann, Nonaxisymmetrically Loaded Solids, University of California at Davis (1968).
9. A. Kalnins, Analysis of Shells of Revolution Subjected to Symmetrical and Nonsymmetrical Loads, JAM, Trans. ASME 31, 467-476 (1964).
10. G. A. Cohen, Computer Analysis of Asymmetric Free Vibrations of Ring Stiffened Orthotropic Shells of Revolution, AIAA J., 3, 2305 - 2312 (1965).
11. P. J. Schroedl, SAVE SS-2, The Babcock and Wilcox Company Report TR 91206, Barberton, Ohio (1969).
12. C. M. Friedrich, SEAL SHELL -2, A Computer Program for the Stress Analysis of a Thick Shell of Revolution with Axisymmetric Pressure, Temperatures, and Distributed Loads, Bettis Atomic Power Laboratory, Pittsburgh, Pa. (1969).
13. J. K. Knowles and E. Reissner, A Derivation of Equation of Shell Theory for Arbitrary Orthogonal Coordinates, J. Math. Phys. 35, 351-358 (1957).
14. H. Kraus, Thin Elastic Shells, John Wiley and Sons, New York, N.Y. (1967).
15. S. Klein, The Cholesky Equation Solver, Report No. ATR-70 (S9990)-2, The Aerospace Corporation, San Bernardino, Cal. (1970).
16. A. Kalnins and J. Lestingi, On the Nonlinear Analysis of Elastic Shells of Revolution, JAM, Trans. ASME 34, 59-64 (1967).
17. T. M. Trainer, L. E. Hulbert, J. F. Lestingi, R. E. Keith, Final Report on the Development of Analytical Techniques for Bellows and Diaphragm Design, AFRPL-TR-68-22 (1968).
18. J. F. Lestingi and L. E. Hulbert, The Application of Linear and Nonlinear Thin Shell Theory in the Analysis of Formed and Welded Metallic Bellows, ASME, 72-WA/PVP-3 (1972).
19. W. C. Kroneke, Classification of Finite Element Stresses According to ASME Section III Stress Categories, submitted for publication.
20. P. P. Bijlaard, Local Stresses in Spherical Shells from Radial or Moment Loadings, The Welding Journal, 36, (1957).
21. J. W. Dally, An Experimental Investigation of the Stresses Produced in Spherical Vessels by External Loads Transferred by a Nozzle, Welding Research Council Bulletin 84 (1963).

TABLE 1

INFLUENCE OF FOURIER HARMONIC NUMBER ON MANIPULATION ERROR FOR H = 0.2 INCHES

TABLE 2

INFLUENCE OF FOURIER HARMONIC NUMBER ON MANIPULATION ERROR FOR H = 0.05 INCHES

TABLE 3

INFLUENCE OF FOURIER HARMONIC NUMBER ON MANIPULATION ERROR FOR H = 0.01 INCHES

SEGMENTS	AXIAL DEFLECTION (x = 20 in) u_x, inch			RADIAL DEFLECTION (x = 20 in) w, inch			AXIAL DEFLECTION (x = 20 in) u_x, inch			RADIAL DEFLECTION (x = 20 in) w, inch			AXIAL DEFLECTION (x = 20 in) u_x, inch			RADIAL DEFLECTION (x = 20 in) w, inch			MACHINE
	Fourier Harmonic Number, n						Fourier Harmonic Number, n						Fourier Harmonic Number, n						
	0	1	2	0	1	2	0	1	2	0	1	2	0	1	2	0	1	2	
5	1.498^{-5}	1.135^{-4}	4.038^{-4}	-9.089^{-4}	-1.297^{-3}	-3.993^{-3}	6.154^{-5}	4.606^{-4}	1.666^{-3}	-7.272^{-3}	-8.832^{-3}	-1.998^{-2}	-3.283^{+1}	-1.981^{+0}	7.002^{+0}	1.187^{+3}	3.990^{+1}	2.778^{+2}	IBM 370/155
10	1.500^{-5}	1.136^{-4}	4.045^{-4}	-9.089^{-4}	-1.297^{-3}	-3.998^{-3}	6.005^{-5}	4.583^{-4}	1.650^{-3}	-7.271^{-3}	-8.838^{-3}	-1.995^{-2}	3.212^{-4}	2.321^{-3}	8.456^{-3}	-8.126^{-2}	-8.904^{-2}	-1.456^{-1}	
20	1.500^{-5}	1.136^{-4}	4.070^{-4}	-9.089^{-4}	-1.297^{-3}	-4.021^{-3}	6.001^{-5}	4.594^{-4}	1.664^{-3}	-7.271^{-3}	-8.843^{-3}	-2.000^{-2}	2.991^{-4}	2.311^{-3}	8.440^{-3}	-8.129^{-2}	-8.920^{-2}	-1.459^{-1}	
40	1.500^{-5}	1.150^{-4}	4.231^{-4}	-9.090^{-4}	-1.304^{-3}	-4.167^{-3}	5.994^{-5}	4.630^{-4}	1.693^{-3}	-7.271^{-3}	-8.857^{-3}	-2.025^{-2}	2.996^{-4}	2.325^{-3}	8.517^{-3}	-8.130^{-2}	-8.929^{-2}	-1.468^{-1}	
100	1.506^{-5}	1.430^{-4}	-1.414^{-4}	-9.116^{-4}	-1.449^{-3}	1.020^{-3}	6.000^{-5}	4.959^{-4}	2.044^{-3}	-7.274^{-3}	-9.018^{-3}	-2.343^{-2}	2.996^{-4}	2.904^{-3}	2.014^{-2}	-8.130^{-2}	-9.177^{-2}	-3.032^{-1}	
200	1.577^{-5}	1.805^{-5}	7.112^{-5}	-9.449^{-4}	-1.220^{-3}	-3.165^{-3}	6.069^{-5}	6.571^{-4}	-1.317^{-3}	-7.334^{-3}	-9.880^{-3}	7.260^{-1}	2.998^{-4}	2.481^{-3}	9.872^{-3}	-8.132^{-2}	-9.995^{-2}	-1.568^{-1}	
5	1.500^{-5}	1.135^{-4}	4.037^{-4}	-9.089^{-4}	-1.297^{-3}	-3.991^{-3}	6.000^{-5}	4.575^{-4}	1.650^{-3}	-7.271^{-3}	-8.829^{-3}	-1.988^{-2}	3.000^{-4}	1.503^{-3}	7.036^{-3}	-8.129^{-2}	-1.744^{-1}	-3.114^{-1}	
10	1.500^{-5}	1.135^{-4}	4.037^{-4}	-9.089^{-4}	-1.297^{-3}	-3.991^{-3}	6.000^{-5}	4.575^{-4}	1.650^{-3}	-7.271^{-3}	-8.835^{-3}	-1.988^{-2}	3.007^{-4}	2.296^{-3}	6.282^{-3}	-8.125^{-2}	-8.902^{-2}	-1.444^{-1}	
20	1.499^{-5}	1.135^{-4}	4.041^{-4}	-9.089^{-4}	-1.297^{-3}	-3.995^{-3}	5.998^{-5}	4.575^{-4}	1.650^{-3}	-7.271^{-3}	-8.835^{-3}	-1.989^{-2}	3.000^{-4}	2.295^{-3}	8.279^{-3}	-8.129^{-2}	-8.914^{-2}	-1.446^{-1}	
40	1.500^{-5}	1.135^{-4}	4.035^{-4}	-9.089^{-4}	-1.297^{-3}	-3.990^{-3}	5.996^{-5}	4.574^{-4}	1.651^{-3}	-7.271^{-3}	-8.835^{-3}	-1.990^{-2}	2.998^{-4}	2.291^{-3}	8.286^{-3}	-8.130^{-2}	-8.914^{-2}	-1.446^{-1}	
100	1.500^{-5}	1.135^{-4}	4.036^{-4}	-9.089^{-4}	-1.297^{-3}	-3.990^{-3}	6.000^{-5}	4.575^{-4}	1.650^{-3}	-7.272^{-3}	-8.836^{-3}	-1.988^{-2}	2.997^{-4}	2.294^{-3}	8.286^{-3}	-8.130^{-2}	-8.914^{-2}	-1.447^{-1}	
200	1.500^{-5}	1.135^{-4}	4.037^{-4}	-9.089^{-4}	-1.297^{-3}	-3.991^{-3}	6.000^{-5}	4.575^{-4}	1.650^{-3}	-7.272^{-3}	-8.836^{-3}	-1.988^{-2}	2.999^{-4}	2.295^{-3}	8.287^{-3}	-8.130^{-2}	-8.915^{-2}	-1.447^{-1}	

Exponents imply a power of ten, e.g. $N^{-m} = N \times (10)^{-m}$ where N is a decimal number.

TABLE 4. COMPARISON OF THEORETICALLY DETERMINED AND EXPERIMENTALLY DETERMINED STRESSES AND STRAINS FOR 3-INCH ONE-PLY TYPE 321 STAINLESS STEEL BELLOWS

			Comparison of Strains[a] microinch/inch		Comparison of Stresses[a] psi	
			Experimental	Theoretical	Experimental	Theoretical
Compression Stresses And Strains	Convolution Crown	Meridional	+401	+484	+14,580	+16,987
		Circumferential	+187	+165	+9,780	+9,887
	Convolution Root	Meridional	+626	+681	+18,963[b]	+20,623
		Circumferential	-	-112	+2,697[b]	+2,935
Internal Pressure Stresses and Strains	Convolution Crown	Meridional	-1295	-1532	-43,500	-50,446
		Circumferential	-232	-171	-19,809	-20,098
	Convolution Root	Meridional	+1833	+1822	+59,064[c]	+58,709
		Circumferential	-	+067	+19,688[c]	+19,559

(a) Calculated and tested for 0.060-in. compression and 50-psi internal pressure.

(b) Calculated on the assumption that $S_1/S_2 = 7.03$

(c) Calculated on the assumption that $S_1/S_2 = 3.00$

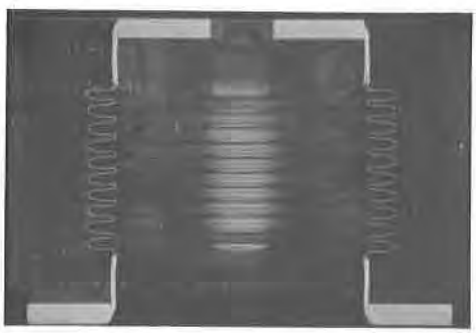

Fig. 1.

CROSS SECTION OF 3-INCH, 1-PLY FORMED TYPE 321 STAINLESS STEEL BELLOWS

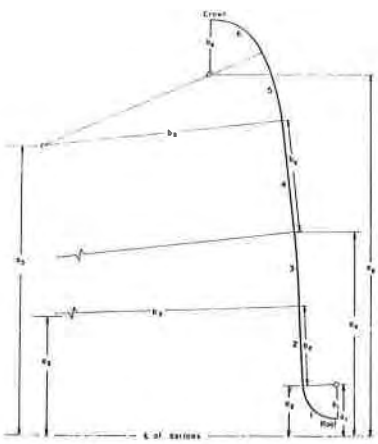

Fig. 2. MATHEMATICAL MODEL OF 3-INCH BELLOWS

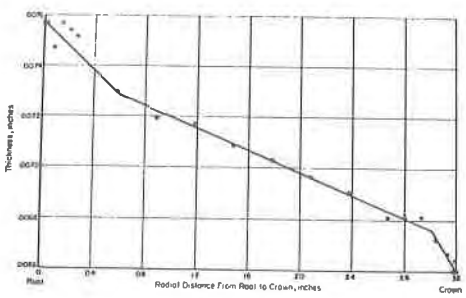

Fig. 3. THICKNESS VARIATION OF 3-INCH BELLOWS

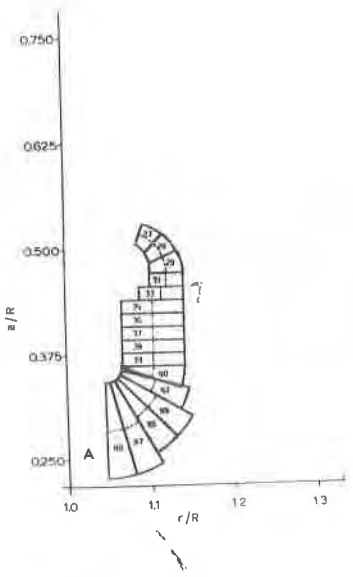

Fig. 4. SAVE SS-2 MODEL OF ESSE SEAL

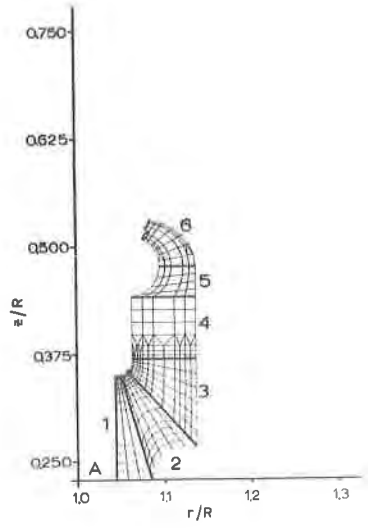

Fig. 5. ABSA AND MONSASTF MODELS OF ESSE SEAL

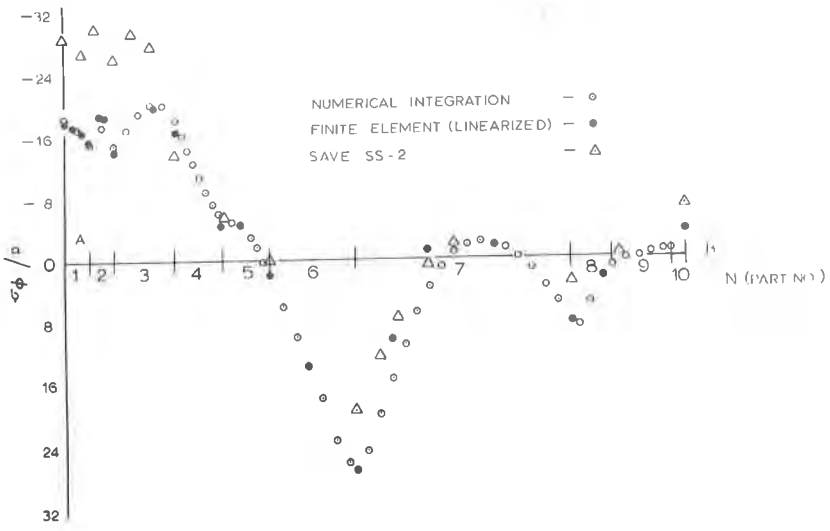

Fig. 6. ESSE SEAL OUTSIDE SURFACE LONGITUDINAL STRESS DISTRIBUTION COMPARISONS

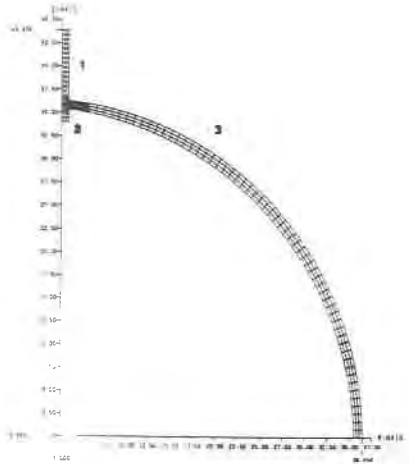

Fig. 7. ALAS AND MONSASTF HEMISPHERE-NOZZLE MODELS

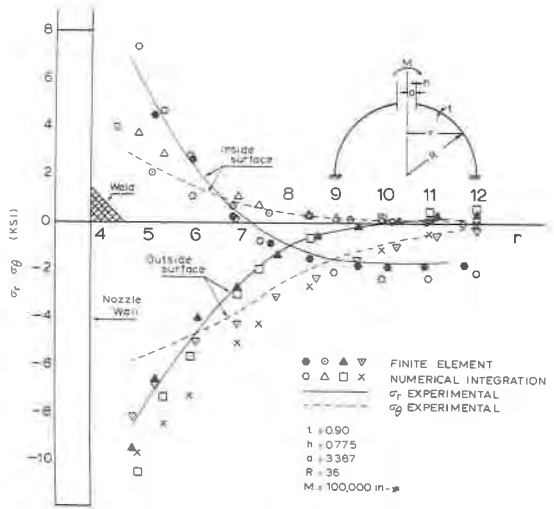

Fig 8. COMPARISON OF EXPERIMENTAL, ALAS, AND MONSASTF STRESS DISTRIBUTIONS FOR FIG. 7 MODEL

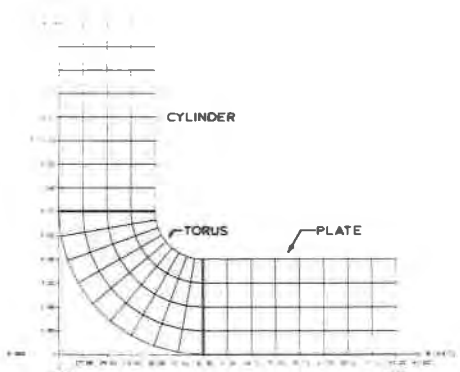

Fig. 9. ALAS AND MONSASTF FLANGE MODELS

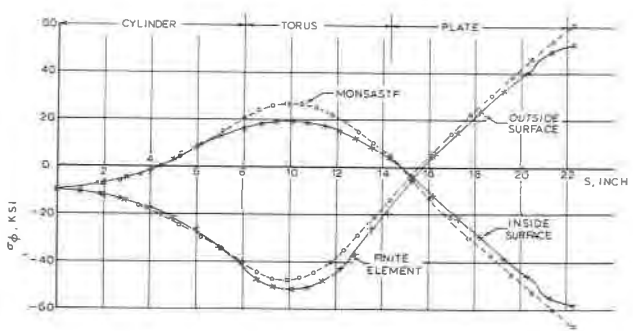

Fig. 10. COMPARISON OF ALAS AND MONSASTF STRESS DISTRIBUTIONS FOR FIG. 9 MODEL